BRAIN
ORIGINAL ARTICLE

Linking lesions in sensorimotor cortex to contralateral hand function in multiple sclerosis: a 7 T MRI study

Mads A. J. Madsen,[1] Vanessa Wiggermann,[1] Marta F. M. Marques,[1] Henrik Lundell,[1] Stefano Cerri,[1,2] Oula Puonti,[1] Morten Blinkenberg,[3] Jeppe Romme Christensen,[3] Finn Sellebjerg[3,4] and Hartwig R. Siebner[1,4,5]

Cortical lesions constitute a key manifestation of multiple sclerosis and contribute to clinical disability and cognitive impairment. Yet it is unknown whether local cortical lesions and cortical lesion subtypes contribute to domain-specific impairments attributable to the function of the lesioned cortex.

In this cross-sectional study, we assessed how cortical lesions in the primary sensorimotor hand area relate to corticomotor physiology and sensorimotor function of the contralateral hand. Fifty relapse-free patients with relapsing–remitting or secondary–progressive multiple sclerosis and 28 healthy age- and sex-matched participants underwent whole-brain 7 T MRI to map cortical lesions. Brain scans were also used to estimate normalized brain volume, pericentral cortical thickness, white matter lesion fraction of the corticospinal tract, infratentorial lesion volume and the cross-sectional area of the upper cervical spinal cord. We tested sensorimotor hand function and calculated a motor and sensory composite score for each hand. In 37 patients and 20 healthy controls, we measured maximal motor-evoked potential amplitude, resting motor threshold and corticomotor conduction time with transcranial magnetic stimulation and the N20 latency from somatosensory-evoked potentials.

Patients showed at least one cortical lesion in the primary sensorimotor hand area in 47 of 100 hemispheres. The presence of a lesion was associated with worse contralateral sensory ($P = 0.014$) and motor ($P = 0.009$) composite scores. Transcranial magnetic stimulation of a lesion-positive primary sensorimotor hand area revealed a decreased maximal motor-evoked potential amplitude ($P < 0.001$) and delayed corticomotor conduction ($P = 0.002$) relative to a lesion-negative primary sensorimotor hand area. Stepwise mixed linear regressions showed that the presence of a primary sensorimotor hand area lesion, higher white-matter lesion fraction of the corticospinal tract, reduced spinal cord cross-sectional area and higher infratentorial lesion volume were associated with reduced contralateral motor hand function. Cortical lesions in the primary sensorimotor hand area, spinal cord cross-sectional area and normalized brain volume were also associated with smaller maximal motor-evoked potential amplitude and longer corticomotor conduction times. The effect of cortical lesions on sensory function was no longer significant when controlling for MRI-based covariates. Lastly, we found that intracortical and subpial lesions had the largest effect on reduced motor hand function, intracortical lesions on reduced motor-evoked potential amplitude and leucocortical lesions on delayed corticomotor conduction.

Together, this comprehensive multilevel assessment of sensorimotor brain damage shows that the presence of a cortical lesion in the primary sensorimotor hand area is associated with impaired corticomotor function of the hand, after accounting for damage at the subcortical level. The results also provide preliminary evidence that cortical lesion types may affect the various facets of corticomotor function differentially.

1 Danish Research Centre for Magnetic Resonance, Copenhagen University Hospital—Amager and Hvidovre, 2650 Hvidovre, Denmark

Received January 04, 2022. Revised May 17, 2022. Accepted May 20, 2022. Advance access publication June 2, 2022

2 Department of Health Technology, Technical University of Denmark, 2800 Kgs Lyngby, Denmark
3 Danish Multiple Sclerosis Center, Department of Neurology, Copenhagen University Hospital—Rigshospitalet, 2600 Glostrup, Denmark
4 Department of Clinical Medicine, University of Copenhagen, 2200 Copenhagen, Denmark
5 Department of Neurology, Copenhagen University Hospital—Bispebjerg and Frederiksberg, 2400 Copenhagen, Denmark

Correspondence to: Hartwig R. Siebner
Kettegard Allé 30
2650 Hvidovre, Denmark
E-mail: h.siebner@drcmr.dk

Keywords: 7 T MRI; multiple sclerosis; cortical lesions; transcranial magnetic stimulation; sensorimotor control

Abbreviations: CL+/– = presence/absence of cortical lesion in the SM1-HAND; CMCT = corticomotor conduction time; CST = corticospinal tract; DWI = diffusion-weighted imaging; EDSS = Expanded Disability Status Scale; FLAIR = fluid-attenuated inversion recovery; FS(p/s) = functional systems (pyramidal/sensory); MEP = motor-evoked potential; MEP_{max} = maximal MEP amplitude; MPRAGE = magnetization prepared rapid gradient echo; RMT = resting motor threshold; SSEP = somatosensory-evoked potential; SM1-HAND = primary sensorimotor hand area; TMS = transcranial magnetic stimulation

Introduction

Multiple sclerosis causes inflammation and demyelination of grey and white matter in the cerebrum and spinal cord.[1] Clinical MRI protocols at field strengths of 1.5 or 3 T readily capture focal inflammation in the white matter, making MRI invaluable for multiple sclerosis diagnosis and monitoring of inflammatory activity.[2] However, cerebral white matter lesion load is only poorly associated with clinical impairment and often fails to explain the individual expression of the numerous symptoms affecting multiple sclerosis patients.[3] Other MRI-based metrics that primarily capture the neurodegenerative component of multiple sclerosis, such as brain and deep grey matter atrophy,[4] cortical thickness[5,6] and spinal cord cross-sectional area,[7] may improve clinical monitoring and decision-making. While these MRI-based metrics primarily relate to global measures of disease-related pathology and disability, markers that reflect disability in a specific functional domain might be more sensitive to disease progression within the relevant brain network.[8–10] Such function-specific markers could help solve the clinico-radiological paradox[11] and improve the diagnostic and prognostic credibility of MRI in multiple sclerosis.

Cortical lesions are both frequent and abundant in all stages of multiple sclerosis.[12] Yet, cortical lesions are difficult to visualize using clinical MRI.[13,14] 7 T MRI provides a supra-linear increase in the signal-to-noise ratio, allowing for a drastic increase in spatial resolution.[15] This has been shown to almost double the detection of cortical lesions,[16] even compared to more specialized sequences on 3 T systems.[17–19] Previous studies have demonstrated that cortical lesion load detected with 7 T MRI correlates with cognitive impairment,[20–23] the Expanded Disability Status Scale (EDSS)[20,21,23–26] and reduced manual dexterity, measured with the 9-hole peg test (9-HPT).[21,22] Cortical lesion load is also associated with disability worsening[26] and disease progression.[27,28] Thus, MRI of cortical lesions bears great potential as a supplementary clinical and prognostic marker in multiple sclerosis. However, to date, 7 T MRI studies have only assessed the clinical impact of whole brain (or supratentorial) cortical lesion load rather than the impact of cortical lesions in a given cortical area on domain-related symptoms.

This study aimed to assess the domain-specific physiological and behavioural consequences of the strategic location of cortical lesions detected at 7 T in patients with multiple sclerosis. Therefore, in addition to assessing sensorimotor behaviour, we recorded motor-evoked potentials (MEPs) and somatosensory-evoked potentials (SSEPs) to test how the underlying cortical pathology of multiple sclerosis affects central sensorimotor physiology.[29] Specifically, we investigated how cortical lesions in the 'hand-knob' area of the primary sensorimotor cortex[30] (SM1-HAND) relate to manual sensory–motor disability and to alterations in excitability and conduction of corticospinal projections to the contralateral hand. The SM1-HAND is the principal cortical input structure and the final cortical output structure of sensorimotor information to and from the hands. Thus, area-specific relationships between the presence and type of cortical lesion and domain-specific dysfunction can be readily uncovered at the behavioural level and with well-established neurophysiological methods (MEP and SSEP), enabling a multifaceted and quantitative assessment of regional cortical function.

We hypothesized that patients with one or more cortical lesion(s) in the SM1-HAND would have (i) higher manual motor and sensory disability; and (ii) reduced integrity of the corticospinal tract (CST) measured with MEPs. We further hypothesized that this would (iii) scale with the number and volume of cortical lesions in the SM1-HAND; and (iv) be in addition to subcortical motor tract damage and whole-brain MRI markers of disability. Finally, we explored the contribution of individual cortical lesion types to behavioural and neurophysiological outcomes. Previous studies have shown the specificity of motor tract damage to motor disability.[8,9] An alternative hypothesis is therefore that brain and spinal cord damage of the sensorimotor tracts are dominating factors of hand disability, because the intact portion of SM1-HAND will effectively compensate for small cortical lesions (in analogy to silent cortical micro-infarcts in patients with stroke). If this was the case, the presence of small cortical lesions should play no or only a marginal role.

Materials and methods

Subjects

We prospectively recruited 50 patients with a diagnosis of either relapsing–remitting (RRMS) or secondary–progressive (SPMS)

multiple sclerosis from the outpatient clinic at the Danish Multiple Sclerosis Center (Copenhagen University Hospital—Rigshospitalet, Copenhagen, Denmark) between August 2018 and September 2020. Exclusion criteria were: age below 18 or above 80 years, clinical relapse, corticosteroid therapy or changes in multiple sclerosis-related medication within 3 months of participation, EDSS above 7, other significant neurologic or psychiatric disorders and contraindications to 7 T MRI. We also recruited 28 age- and sex-matched healthy controls with no significant neurological or psychiatric disorders, no history of cerebral haemorrhage or brain damage, no major medical morbidities and no contraindications to 7 T MRI. A subset of 37 patients and 20 healthy volunteers participated in a neurophysiological experiment, including SSEP and MEP measurements. These participants were screened for contraindications to transcranial magnetic stimulation (TMS).[31] All participants gave informed written consent prior to participation. The study was approved by the local ethics committee (H-17033372) and monitored by the local good clinical practice unit. The study complied with the Helsinki declaration of human experimentation and was preregistered at www.clinicaltrials.gov (ID: NCT03653585).

Experimental design

Data collection for this prospective cross-sectional study consisted of three experimental sessions conducted within a month. Measurements on the first day consisted of behavioural and clinical examinations and structural whole-brain MRI at 7 T. On the second day, we obtained diffusion-weighted 7 T MRI images. On the third day, we performed neurophysiological examinations of the sensorimotor cortex and its connectivity to the contralateral hand using TMS and SSEPs. None of the participants experienced any relapses during their participation in the experiment.

MRI data acquisition

MRI data were collected on a 7 T Philips Achieva scanner with a dual transmit, 32-channel receive head coil (Nova Medical). The structural whole-brain MRI protocol consisted of: (i) a magnetization prepared (MP) fluid-attenuated inversion recovery (FLAIR); (ii) T_1-weighted MP rapid gradient echo (MPRAGE); (iii) magnetization prepared 2 rapid gradient echo (MP2RAGE); (iv) T_2-weighted turbo spin echo (TSE); and (v) a T_1-weighted sequence. Prospective fat-navigated motion correction[32] was applied during all scans, except the T_1-weighted. In addition, multislice diffusion-weighted imaging (DWI) data were collected over 32 diffusion gradient directions. Detailed sequence parameters are listed in Supplementary Table 1.

MRI data processing

MRI preprocessing

All structural images were bias-field corrected in SPM12 (https://www.fil.ion.ucl.ac.uk/spm/software/spm12/) using parameters optimized for 7 T MRI.[33] The MPRAGE image was skull-stripped, rigidly aligned and resampled to the 0.5 mm^3 MNI-space template. The bias-field corrected FLAIR, T_2- and T_1-weighted images were linearly co-registered to the MPRAGE image using *spm_coreg*. MP2RAGE image calculation was adapted to the inversion times of our sequence. MP2RAGE images were computed by subtraction of the first inversion image from the second and by dividing the resulting image by the sum of both inversion images. MP2RAGE contrast images were affinely co-registered to individual resampled MPRAGE images using *antsRegistationSyn*.[34]

Lesion segmentation

Cortical and white matter lesion masks were manually and independently created by three experienced readers (H.C.A.S., M.A.J.M. and S.G.). All readers were blinded to participants' demographic and clinical status. Lesions were identified using FLAIR as the primary image, supported by MPRAGE and T_2-weighted images. Segmentations were carried out using either FSLeyes (v.0.34.2, FMRIB, Oxford, UK) or Jim (v.7.0, Xinapse, Essex, UK). Consensus recommendations for cortical lesion segmentation are only available for double inversion recovery images acquired at 1.5 or 3 T.[35] Therefore, we defined cortical lesions similar to previous publications[36,37] as: (i) clearly hyper- (FLAIR, T_2-weighted) or hypointense (MPRAGE); (ii) visible on at least two sequences; and (iii) spanning at least three voxels on two consecutive (axial) slices. Signal abnormalities with a linear or tubular appearance were classified as vessels and not drawn. Forty subjects were randomly selected to establish joint consensus among readers. For this purpose, all drawn regions were re-examined and classified according to the system proposed by Bø *et al.*[38] as either: (i) white matter; (ii) juxtacortical, confined to the white matter on all sequences but touching the grey–white matter boundary; (iii) type I leucocortical, located in both grey and white matter on at least one sequence; (iv) type II intracortical, confined to the cortical grey matter, not touching the pial surface on any sequence; or (v) type III/IV subpial, confined to the cortical grey matter and touching the pial surface on at least one sequence. Based on the joint consensus, M.A.J.M. classified lesions in the remaining 38 subjects. Manual modification of lesion segmentations was carried out by H.C.A.S. or M.A.J.M. Fig. 1A illustrates the appearance of different cortical lesion subtypes on the used sequences.

Cortical surface reconstruction, parcellation and volumetric estimation

Surface reconstruction, volumetric segmentation and cortical thickness estimation was carried out using *freesurfer* version 7.1.1 (http://surfer.nmr.mgh.harvard.edu/). *Samseg* segmentation[39] with lesion extension[40] was performed on MP2RAGE, T_1-weighted, T_2-weighted and FLAIR images with the *–use-t2w* flag. For four subjects, a T_2-weighted scan was not available and segmentation was performed without. This did not seem to bias segmentations. Topographical defects in the white and pial surface due to juxtacortical or white matter lesions were corrected by lesion filling. All surfaces were carefully inspected and manual corrections were made if required. The temporal lobes were excluded from volumetric analyses in the current study due to low signal-to-noise ratio in some participants.

Defining the sensorimotor hand knob as region of interest

To determine the role of area-specific cortical lesions on sensorimotor performance, an experienced reader (M.A.J.M.) identified the hand-knob bilaterally on individual MPRAGE images. The hand-knob is an anatomical landmark situated in the precentral gyrus in which hand motor function is represented.[30] A spherical region of interest with a diameter of 30 mm was centred on the right and left hand-knob to cover both primary sensory and motor hand areas (Fig. 1B and Supplementary Fig. 1). The size of the sphere was determined based on previous estimations of the maximal

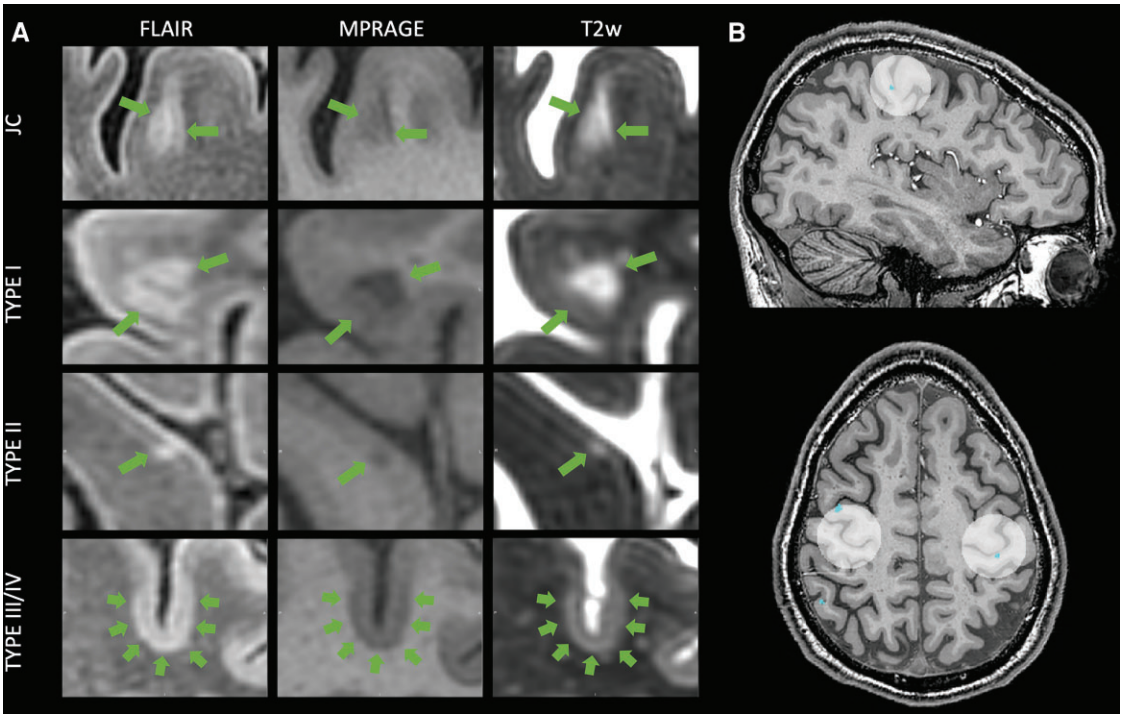

Figure 1 7 T depiction of cortical lesion subtypes and sensorimotor hand knob regions of interest. (**A**) Representable depiction of the appearance of the three different cortical lesion subtypes and a juxtacortical lesion on the three high-resolution scans used for cortical lesion detection. (**B**) Visualization of the hand knob regions of interest including two segmented intracortical lesions. JC = juxtacortical; T2w = T_2-weighted.

hand-knob size[30] and in order to include both the pre- and postcentral cortices. We chose a manual approach because the hand knob is heterogeneously distributed along the precentral gyrus and because, to our knowledge, no atlas currently incorporates an SM1-HAND region. The region of interest was limited to only include Broadmann areas 1, 2, 3a, 3b, 4a, 4p and 6 derived from *freesurfer* segmentations (Supplementary Fig. 1). The cortical lesion number and volume in these regions of interest were calculated per hemisphere.

In order to assess the spatial specificity of our results we also investigated two control regions of interest. The first region of interest was the paracentral area derived from the Desikan–Killiany atlas from freesurfer segmentations. This area comprises mainly of leg and genital sensorimotor representations and was chosen as a within-domain control region. Additionally, we choose a non-sensorimotor area with a more similar composition of cortical lesions as the SM1-HAND region of interest, namely the caudal middle frontal area from the Desikan–Killiany atlas.

Diffusion-weighted imaging and lesion volumes of the corticospinal tract

DWI data were available for 67 participants (22 healthy controls and 45 patients) due to dropout between the first and second experimental day. DWI data were processed using FSL[41] and MRtrix.[42] All imaging volumes were denoised,[43] corrected for field inhomogeneities with *topup*[44] and eddy current and slice-to-volume corrected with *eddy_cuda*.[45] Two regions of interest covering the right and left CST were extracted using the TractSeg toolbox[46] and cut at the brainstem level, determined by individual *freesurfer* segmentations. To compute the lesion fraction of the CST, T_2-weighted images were affinely transformed to DWI space of each subject with *antsRegistrationSyn*. Lesion masks were mapped to DWI space using nearest-neighbour interpolation. For four subjects without T_2-weighted images, FLAIR images were used instead. To extend our analysis to subjects without DWI data, all CST regions of interest were mapped onto a study-specific T_1-weighted template generated with *antsMultivariateTemplateConstruction2*.[34] The CST template was thresholded at 40% overlap, as this threshold resulted in the largest dice coefficients between the template and original segmentations of six randomly selected participants. Template CSTs were warped to individual MPRAGE images (*antsApplyTransform*) and CST lesion fractions of subjects that did not have DWI data were estimated in this space.

Infratentorial lesion volume (brainstem and cerebellum) was calculated from *freesurfer* segmentations by back-transforming these regions to subject space using *mri_label2vol* and overlaying the respective lesion masks.

Spinal cord cross-sectional area

Spinal cord cross-sectional area was assessed using the SpinalCordToolbox.[47] Spinal cords were segmented on MPRAGE images using *sct_deepseg_sc*. Segmentations were individually reviewed by two readers (H.C.A.S. and V.W.) and manually corrected (V.W.) if needed. The intersection between C2 and C3 was manually labelled to aid the identification of cervical spinal cord levels. If signal loss in the spinal cord area was too significant on MPRAGE, T_1-weighted images were used instead. Spinal cord cross-sectional area was computed across the C1/C2 segment using *sct_process_segmentation*.

Clinical and behavioural examination

EDSS, pyramidal (FSp) and sensory (FSs) functional systems scores were obtained from patient clinical records if assessed within 3 months of enrolment. Otherwise, EDSS was determined on the second day of MRI. Manual dexterity was assessed on both hands with the 9-HPT,[48] the Jebsen Taylor hand function test (JTHFT)[49] and a finger tapping task in which maximum tapping rates of each individual finger were measured over a 10-s period and responses for each hand were averaged over all digits. The results from the 9-HPT, JTHFT and finger tapping were Z-scored relative to data from the healthy participants, separately for each hand. A composite motor score for each hand was then calculated as the mean Z-score over the three tests. Motor fatigue was assessed from the fatigue scale for motor and cognitive functions (FSMC)[50] and handedness was tested using the Edinburgh handedness inventory with participants' hand dominance assigned based on positive (right-handed) or negative values.[51]

Sensory acuity was assessed using the grating orientation discrimination task (GODT).[52,53] Grating widths descending from 3 to 2, 1.5, 1, 0.75 and 0.5 mm were applied in either longitudinal or transverse direction to the distal pad of the index and little finger of the right and left hand by an experimenter. Gratings were applied 15 times in each direction in a pseudo-randomized order. Testing ended when performance dropped below 75% of correct responses. Performance was calculated as:

$$Threshold = G_{low} + \left(\frac{0.75 - P_{low}}{P_{above} - P_{low}}\right) * (G_{above} - G_{low}) \quad (1)$$

with G = grating width, P = % correct trials, low = lowest grating tested, above = grating width above *low* similar to Ragert *et al.*[53] If participants failed at the largest grating width, performance was calculated as:

$$Threshold = G_{low} + \left(\frac{0.75 - P_{low}}{P_{low}}\right) * (G_{low}) \quad (2)$$

If participants scored below 50% chance level, P_{low} was set to 50%, setting a ceiling effect of 4.5 mm in the test. Additionally, we assessed sensory deficits by applying light touch and a dull/sharp discrimination test to each individual digit. The digit sensory deficit score (SDS) was quantified on the ordinal scale of the superficial sensation test of the EDSS. Responses for each test were averaged across digits within each hand. Analogously to the assessment of motor hand function, we calculated a composite sensory score on the GODT and the SDS. Due to the non-normal distribution of data, we performed a principal component analysis on scaled and centred variables from all participants.

Neurophysiological recordings

MEPs were recorded from the first dorsal interosseous muscle from which we obtained the maximal MEP amplitude (MEP_{max}) during contraction.[54] The corticomotor conduction time (CMCT) was calculated based on the F-wave method[54] and resting motor threshold (RMT) was measured as suggested by Rossini *et al.*[55] Lastly, we determined the N20 latency from SSEPs, elicited from peripheral digital nerve stimulation of the index finger and recorded with scalp EEG electrodes. The neurophysiological measurements and analyses are described in detail in the Supplementary material.

Statistical analysis

Statistical analysis was carried out in R (R-core team, 2021) and linear mixed-effects modelling was performed using the packages *lme4*, *multcomp* and the *step* function from the package *lmerTest*.

Descriptive statistics

Patients were grouped based on the presence or absence of cortical lesions in the SM1-HAND region of interest (CL+, CL–, respectively). Grouping was done separately for the dominant and non-dominant hemisphere and for the whole brain when comparing non-lateralized variables. Group differences between healthy participants and patient groups for metrics not specific to multiple sclerosis were assessed using Kruskal–Wallis and *post hoc* Mann–Whitney U-tests. Disease-specific variables were compared between the patient groups using Mann–Whitney U-tests and chi-square tests for categorical data. *P*-values were corrected for multiple comparisons using the Holm method.

Impact of SM1-HAND cortical lesions on manual sensory–motor function and neurophysiological measures

We used linear mixed-effects models to compare outcome measures between three groups: Healthy controls, CL+ patients and CL– patients. A mixed-effects design was chosen to include data from both the dominant and non-dominant hand/hemisphere in the models. Fixed effects included Group, Sex, Age and (hand) Dominance to account for differences in performance of the dominant and the non-dominant hand, and Subject as a random factor with random intercept. The effect of Group was assessed with likelihood ratio tests of the full model against the model without Group. *Post hoc* comparisons were performed with Tukey's honest significance tests. *P*-values were corrected for multiple comparisons using the Holm method. Identical analyses were conducted using the paracentral and caudal middle frontal control regions of interest.

In order to ensure the added contribution of SM1-HAND cortical lesions on the outcome measures showing a significant Group effect, we also conducted step-wise backwards linear mixed-effects models. All models considered the following variables for stepwise deletion:

$$\begin{aligned} &Outcome\ variable \sim group + hand\ dominance + normalized\ brain\ volume \\ &+CST\ white\ matter\ lesion\ fraction + pericentral\ cortical\ thickness \\ &+spinal\ cord\ cross\ sectional\ area + whole\ brain\ cortical\ lesion\ number \\ &+infratentorial\ lesion\ volume + sex + age + (1|subject) \end{aligned}$$

In this analysis, only patient data were included (i.e. group: CL+ and CL–). Lateralized MRI measures were considered in the contralateral hemisphere relative to the dominant and non-dominant hand. A step-wise procedure was conducted with backward elimination, only on fixed effects. *P*-values were calculated from *F*-tests based on Satterthwaite's approximation, and the *P*-value for inclusion was set to $P < 0.1$ in order to include contributions of non-significant effects on the beta coefficients.

Exploratory analysis of cortical lesion subtypes

To explore the contribution of cortical lesion subtypes on our outcome measures, the final model obtained from the stepwise

Table 1 Global participant demographics, clinical characteristics and MRI measures

Patients				
	HC ($n = 28$)	CL− ($n = 21$)	CL+ ($n = 29$)	All patients ($n = 50$)
Demographics				
Age, years, mean (SD)	44.0 (14.3)	39.1 (9.83)	49.5 (11.9)	45.1 (12.1)
Sex, *n* (% female)	19 (67.9%)	15 (71.4%)	18 (62.1%)	33 (66.0%)
MS phenotype, *n* (% RRMS)	—	18 (85.7%)	19 (65.5%)	37 (74.0%)
EDSS, median [min, max]	—	3.00 [0, 6.50]	3.50 [1.50, 6.50]	3.50 [0, 6.50]
FS pyramidal, median [min, max]	—	1.00 [0, 3.00]	**2.00 [0, 4.00]**[a]	2.00 [0, 4.00]
Missing (*n*)	—	0	1 (3.4%)	1 (2%)
FS sensory, median [min, max]	—	1.00 [0, 2.00]	2.00 [0, 3.00]	1.00 [0, 3.00]
Massing (*n*)	—	—	1 (3.4%)	1 (2%)
Disease duration, median [min, max]	—	6.00 [0, 24.0]	**13.5 [1.00, 35.0]**[a]	10.0 [0, 35.0]
Motor fatigue, median [min, max]	—	21.0 [0, 30.0]	21.0 [5.00, 38.0]	21.0 [0, 38.0]
Lesion and MRI measures				
Total cortical lesions, # mean (SD)	—	8.33 (10.6)	**31.2 (24.1)**[a]	21.6 (22.6)
# median [min, max]	—	4.00 [0, 44.0]	**24.0 [2.00, 98.0]**[a]	15.5 [0, 98.0]
Type I, # mean (SD)	—	5.43 (7.68)	14.1 (16.4)	10.5 (14.0)
# median [min, max]	—	2.00 [0, 32.0]	7.00 [0, 63.0]	6.50 [0, 63.0]
Type II, # mean (SD)	—	1.81 (2.32)	**10.5 (8.53)**	6.84 (7.90)
# median [min, max]	—	1.00 [0, 9.00]	**8.00 [1.00, 33.0]**[a]	5.00 [0, 33.0]
Type III/IV, # mean (SD)	—	1.10 (1.30)	**6.62 (8.01)**	4.30 (6.70)
# median [min, max]	—	1.00 [0, 9.00]	**8.00 [1.00, 33.0]**[a]	5.00 [0, 33.0]
Juxtacortical lesions, # mean (SD)	—	7.29 (10.6)	15.8 (15.3)	12.2 (14.1)
# median [min, max]	—	2.00 [0, 37.0]	8.00 [0, 45.0]	6.00 [0, 45.0]
White matter lesion volume, cm^3 mean (SD)	—	8.24 (15.1)	12.3 (13.2)	10.6 (14.0)
cm^3 median [min, max]	—	2.19 [0.1, 59.4]	8.58 [0.38, 60.7]	4.48 [0.1, 60.7]
Infratentorial lesion volume, cm^3 mean (SD)	—	0.103 (0.195)	0.116 (0.182)	0.111 (0.185)
cm^3 median [min, max]	—	0.016 [0, 0.65]	0.057 [0, 0.76]	0.046 [0, 0.76]
Spinal cord CSA, mm^2 mean (SD)	62.0 (7.13)	60.6 (7.80)	**54.9 (10.1)**[a,b]	57.3 (9.57)
Normalized brain volume, % ICV mean (SD)	60.7 (2.67)	61.0 (5.53)	**56.3 (5.18)**[a,b]	58.3 (5.77)

CL− = patients with no cortical lesion in either handknob region of interest; CL+ = patients with one or more cortical lesions in one or both handknob regions of interest; CSA = cross-sectional area; MS = multiple sclerosis; RRMS = elapsing–remitting multiple sclerosis.
Significant values are highlighted in bold.
[a]$P < 0.05$ between CL− and CL+.
[b]$P < 0.05$ between healthy controls and patient group.

regression analysis was modified to include patient dichotomization for the three cortical lesion subtypes. Thus, the reassessed model included three Group variables (i.e. type I+/−, type II+/−, type III/IV+/−). Additionally, we explored Spearman's rank correlations between the outcome measures and cortical lesion volume and number for each lesion subtype and all cortical lesions in the SM1-HAND. These correlations were performed in CL+ patients only.

Correlations with disability

In patients, associations between disability, neurophysiological measures and MRI metrics were tested with Spearman's rank correlations in order to investigate the replicability of previous studies. Bilateral measures were averaged between hands/hemispheres when tested against non-lateralized measures of disease severity or MRI metrics. Correlations with disability were corrected for multiple comparisons by the number of tests conducted for each outcome variable using the Holm method.

All models were assessed for normality and heteroscedasticity by visual inspection of residual and quartile-quartile plots. Outcome variables were transformed if required. To compare the effects of different MRI variables from the stepwise regression models, standardized β-coefficients and 95% confidence intervals (CI) are reported. All tests were two-sided and an alpha level of $P < 0.05$ was considered statistically significant. Participants with missing data were excluded from the corresponding analysis.

Data availability

The pseudonymized data can only be shared with a formal Data Processing Agreement and a formal approval by the Danish Data Protection Agency in line with the requirements of the GDPR.

Results

Cortical lesions detected with 7 T MRI

Forty-six of the 50 patients showed cortical lesions on 7 T MRI, with a median of 15.5 (range: 0–98) lesions per patient (Table 2). Twenty-nine patients (58%) had cortical lesion(s) in the SM1-HAND region of interest of either one or both hemispheres and were classified as 'CL+' patients. Of these, 22 patients (76%) had cortical lesions in the dominant SM1-HAND and 25 patients (86%) in the non-dominant SM1-HAND. Eighteen patients (62%) had a cortical lesion in both SM1-HAND regions of interest. These patients are represented as CL+ in both the dominant and non-dominant groups. The median lesion count for CL+ patients in the SM1-HAND area was 1 (range 1–5). In the paracentral control region

Table 2 Lateralized sensory and motor performance and MRI measures

	Dominant hand/hemisphere				Non-dominant hand/hemisphere			
	HC ($n = 28$)	CL− ($n = 28$)	CL+ ($n = 22$)	All patients ($n = 50$)	HC ($n = 28$)	CL− ($n = 25$)	CL+ ($n = 25$)	All patients ($n = 50$)
Sensory and motor tests								
9-HPT, mean (SD)	16.7 (2.01)	**20.3 (4.77)**[a]	**22.1 (6.01)**[a]	21.1 (5.37)	17.9 (2.01)	**19.5 (3.14)**[a]	**27.2 (9.21)**[a,b]	23.4 (7.84)
JTHFT, mean (SD)	38.4 (6.30)	**48.2 (11.4)**[a]	**52.6 (14.9)**[a]	50.1 (13.1)	60.6 (11.5)	**71.1 (14.1)**[a]	**89.5 (23.0)**[a,b]	80.3 (21.1)
Finger tapping, mean (SD)	48.3 (4.84)	45.0 (8.06)	42.2 (7.92)	43.7 (8.04)	43.8 (5.09)	42.4 (5.15)	**34.9 (9.13)**[a,b]	38.6 (8.25)
Sensory deficit score, mean (SD)	0.03 (0.12)	**0.79 (0.92)**[a]	**0.91 (1.08)**[a]	0.85 (0.99)	0.01 (0.038)	**0.53 (0.71)**[a]	**1.15 (1.04)**[a,b]	0.845 (0.940)
Missing, *n* (%)	0	1 (3.6%)	0	1 (2%)	0	1 (4%)	0	1 (2%)
GODT, mean (SD)	2.90 (0.788)	3.23 (1.02)	**3.80 (0.886)**[a]	3.47 (0.996)	2.67 (0.811)	2.84 (0.988)	**3.95 (0.563)**[a,b]	3.38 (0.977)
Missing, *n* (%)	0	0	1 (4.5%)	1 (2%)	0	1 (4%)	2 (8%)	3 (6%)
MRI measures								
CST WM lesion fraction, % mean (SD)	—	0.942 (1.86)	1.28 (1.92)	1.09 (1.87)	—	0.703 (1.46)	1.32 (2.43)	1.01 (2.01)
% median [min, max]	—	0.102 [0, 7.64]	0.554 [0, 8.13]	0.288 [0, 8.13]	—	0.223 [0, 5.53]	0.711 [0, 11.6]	0.287 [0, 11.6]
Pericentral CTh, mm, mean (SD)	2.60 (0.088)	2.55 (0.105)	**2.50 (0.111)**[a]	2.53 (0.109)	2.55 (0.0862)	2.54 (0.092)	**2.46 (0.126)**[a,b]	2.50 (0.116)

9-HPT = 9-hole peg test; CL− = patients with no cortical lesion in the contralateral handknob region of interest; CL+ = patients with one or more cortical lesions in the contralateral handknob region of interest; CTh = cortical thickness; GODT = grating orientation discrimination task; HC = healthy control; JTHFT = Jebsen Taylor hand function test; SD = standard deviation; WM = white matter.

Significant values are highlighted in bold.

[a]$P < 0.05$ between healthy controls and patient group.

[b]$P < 0.05$ between CL− and CL+.

of interest there were 28 CL+ hemispheres and in the caudal middle frontal control region of interest there were 41 CL+ hemispheres.

In healthy controls, cortical hyperintensities were rare. We found seven cortical hyperintensities in five healthy controls (range: 0–2; Supplementary Fig. 2). This amount would correspond to a false positive rate of 0.65%, provided that these cortical hyperintensities represent false positives. None of these cortical hyperintensities were in the SM1-HAND.

Clinical characteristics

Population demographics, MRI and clinical information are presented in Tables 1 and 2. There were no differences in age and sex composition between healthy controls and patients. Both patient groups performed worse than healthy controls in all sensory and motor tests on both hands, with the exception of finger tapping for the dominant hand and GODT for CL− patients. Notably, CL+ patients performed significantly worse than CL− patients in all tasks, but the effect was only statistically significant for the non-dominant hand. Additionally, CL+ patients had lower normalized brain volumes, spinal cord cross-sectional area and pericentral cortical thickness of the non-dominant hemisphere. CL+ patients had a higher FSp score, longer disease duration and more whole-brain cortical lesions, with significantly more type II and III/IV lesions. From the principle component analysis of sensory tests, the first principal component explained 71% of variance for the dominant hand and 72.8% of variance for the non-dominant hand and was used as the composite sensory score.

Lesions in SM1-HAND and contralateral hand function

In both patient groups, sensory [$\chi^2(2) = 30.57$, $P < 0.001$] and motor [$\chi^2(2) = 28.26$, $P < 0.001$] function of the hand was reduced compared to healthy controls. Additionally, cortical lesions in the SM1-HAND was associated with poorer motor (mean ± standard error: 0.86 ± 0.33, $z = 2.61$, $P = 0.009$) and sensory (0.49 ± 0.2, $z = 2.45$, $P = 0.014$) function of the contralateral hand compared with patients without a lesion (Fig. 2A and B) and healthy controls (motor: 2.16 ± 0.36, $z = 5.94$, $P < 0.001$, sensory: 1.38 ± 0.22, $z = 6.2$, $P < 0.001$). CL− patients also performed worse than healthy controls (motor: 1.3 ± 0.35, $z = 3.72$, $P < 0.001$, sensory: 0.89 ± 0.22, $z = 4.12$, $P < 0.001$).

Linear mixed models using the control regions of interest did not reveal any differences between CL+ and CL− patients for motor or sensory performance ($P > 0.28$; Supplementary Tables 4 and 5). Prompted by the observation that motor performance of CL+ patients seemed more affected on the non-dominant side, we performed a *post hoc* follow-up analysis not specified in the pre-registration, including an interaction term between Group and Dominance. Here we found a significant Group × Dominance interaction [$\chi^2(2) = 6.74$, $P = 0.034$] for the composite motor score. *Post hoc* tests revealed a difference in motor performance between CL+ and CL− patients only for the non-dominant hand ($P = 0.003$; Supplementary Fig. 3).

The statistical effect of SM1-HAND lesions on contralateral motor hand function remained significant after stepwise variable reduction of other variables of interest, including normalized brain volume, white matter lesion fraction of the CST, pericentral cortical thickness, spinal cord cross-sectional area, whole-brain cortical lesion number and infratentorial lesion volume. Notably, only covariates related to the sensorimotor system were retained from the stepwise mixed linear regression model comparing CL+ and CL−

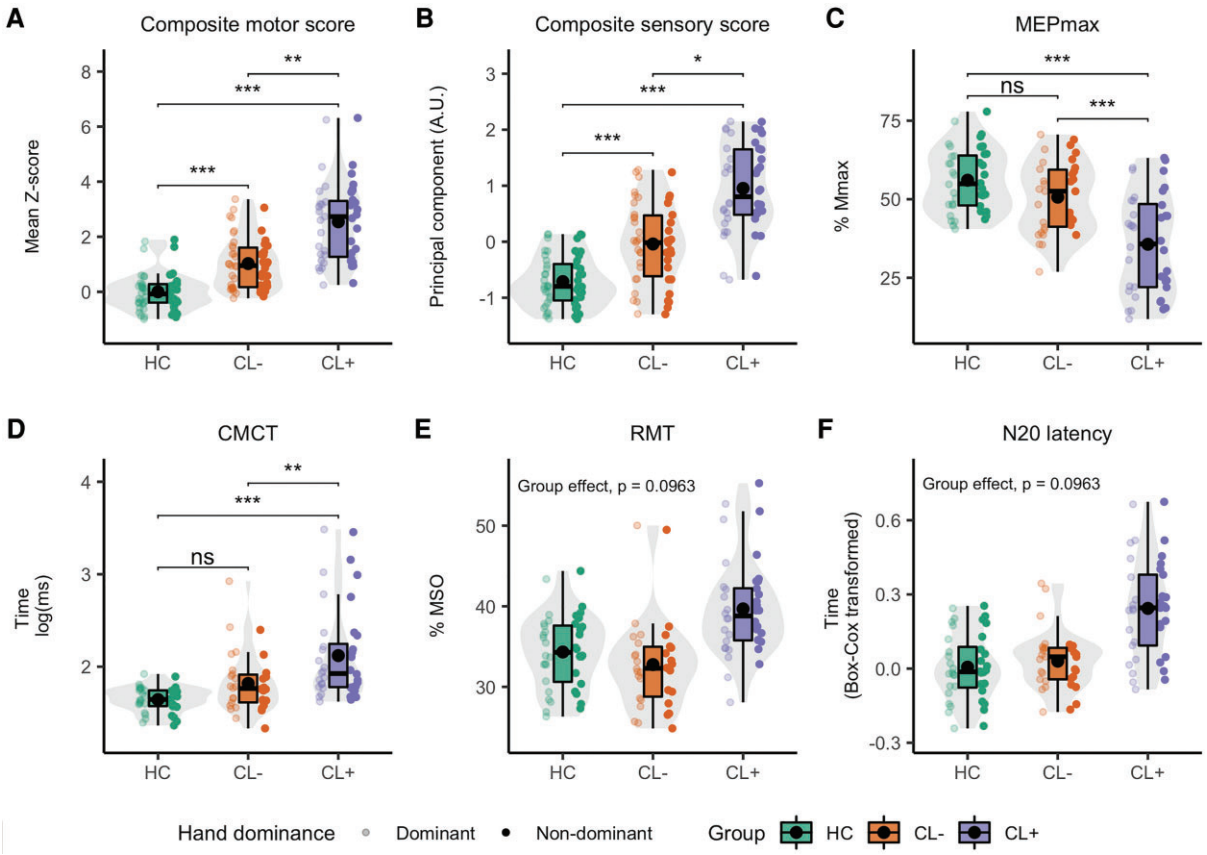

Figure 2 Predicted behavioural and neurophysiological measures. Box and violin plots of predicted values from the mixed linear models for healthy controls and patients with (CL+) and without cortical lesions (CL–) in the contralateral hand knob region of interest. (**A**) Composite motor score; (**B**) composite sensory score; (**C**) MEP_{max}; (**D**) CMCT; (**E**) RMT; (**F**) N20 latency. Box plots include median and interquartile range as horizontal lines and the mean as a black dot. Whiskers indicate the 5th and 95th percentiles. Individual predicted data-points are plotted on either side of the box plot, with low opacity representing the dominant hand and high opacity the non-dominant hand. $^{*}P < 0.05$, $^{**}P < 0.01$, $^{***}P < 0.001$, ns = not significant.

patients. In addition to Group [CL+ versus CL– patients, $t(91.60) = 2.83$, $P = 0.006$], white matter lesion fraction of the CST [$t(59.76) = 3.41$, $P = 0.001$], spinal cord cross-sectional area [$t(50.69) = -3.34$, $P = 0.002$] and infratentorial lesion volume [$t(49.29) = 2.34$, $P = 0.023$] were associated with composite motor scores (conditional $R^2 = 0.583$). For the composite sensory score, Group [$t(93.57) = 1.7$, $P = 0.097$], *age* [$t(50.13) = 2.26$, $P = 0.028$], spinal cord cross-sectional area [$t(47.73) = -1.74$, $P = 0.088$] and infratentorial lesion volume [$t(47.67) = 2.38$, $P = 0.021$] were retained in the final model (conditional $R^2 = 0.651$; Fig. 3A and B).

Lesions in SM1-HAND and sensorimotor physiology

A summary of the subpopulation of healthy controls and patients that underwent neurophysiological examinations is provided in Supplementary Table 2. Apart from CMCT, all neurophysiological outcome measures correlated with the composite motor and sensory scores (Table 3).

Examinations of the corticomotor pathway with TMS showed that cortical lesions in SM1-HAND were associated with a reduced maximal amplitude of the motor-evoked response in the contralateral hand [$\chi^2(2) = 22.6$, $P < 0.001$]. *Post hoc* tests showed that CL+ patients had lower MEP_{max} than healthy controls and CL– patients (-19.72 ± 4.5, $z = -4.38$, $P < 0.001$ and -14.64 ± 3.65, $z = -4.01$, $P < 0.001$, respectively). There was no significant difference between CL– patients and healthy controls ($P = 0.26$). SM1-HAND cortical lesions were associated with prolonged log-transformed CMCT [$\chi^2(2) = 17.4$, $P < 0.001$], with CL+ patients having longer conduction times than healthy controls (0.45 ± 0.12, $z = 3.85$, $P < 0.001$) and CL– patients (0.26 ± 0.08, $z = 3.24$, $P = 0.002$). Using the RMT as a proxy for cortical excitability, we did not find any statistically significant differences between Groups [$\chi^2(2) = 4.78$, $P = 0.096$] after controlling for multiple comparisons (Fig. 2C–F). Sensory–cortical conduction time from the hand to the contralateral SM1-HAND was quantified with the N20 latency, calculated from SSEP recordings. Patients with a highly delayed cortical N20 latency all belonged to the CL+ group (Fig. 2F), but the effect of Group on Box–Cox transformed N20 latency was not significant [$\chi^2(2) = 6.07$, $P = 0.096$] after controlling for multiple comparisons.

Linear mixed models using the control regions of interest did not reveal any significant differences between CL+ and CL– patients for any neurophysiological measures ($P > 0.05$; Supplementary Tables 4 and 5).

Following stepwise regression, cortical lesions in SM1-HAND was still associated with a reduced MEP_{max} [$t(73.34) = -3.5$, $P = 0.001$] after accounting for the effects of spinal cord atrophy [$t(37.20) = 4.27$, $P < 0.001$], normalized brain volume [$t(38.6) = -3.58$, $P = 0.001$] and *age* [$t(37.69) = -1.88$, $P = 0.068$] (conditional $R^2 = 0.696$). Normalized brain volume [$t(38.78) = 2.91$ $P = 0.006$], spinal cord cross-sectional area [$t(37.53) = -4.74$, $P < 0.001$] and

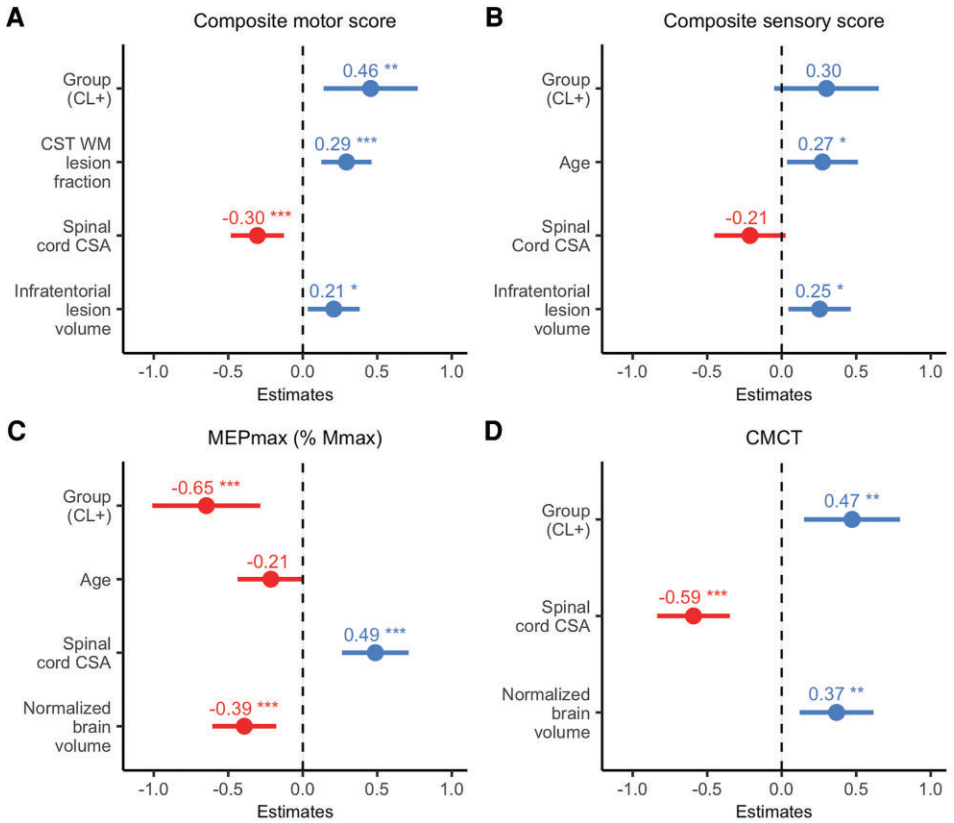

Figure 3 Stepwise mixed linear regression models. Standardized β-coefficients (dots) and 95% standardized CIs of effect size (lines) are plotted for each variable included from the stepwise mixed linear regression models. (**A**) Composite motor score; (**B**) composite sensory score; (**C**) MEP_{max}; (**D**) CMCT. Negative and positive values denote a negative and a positive relationship, respectively. $^{*}P < 0.05$, $^{**}P < 0.01$, $^{***}P < 0.001$. WM = white matter; CSA = cross-sectional area.

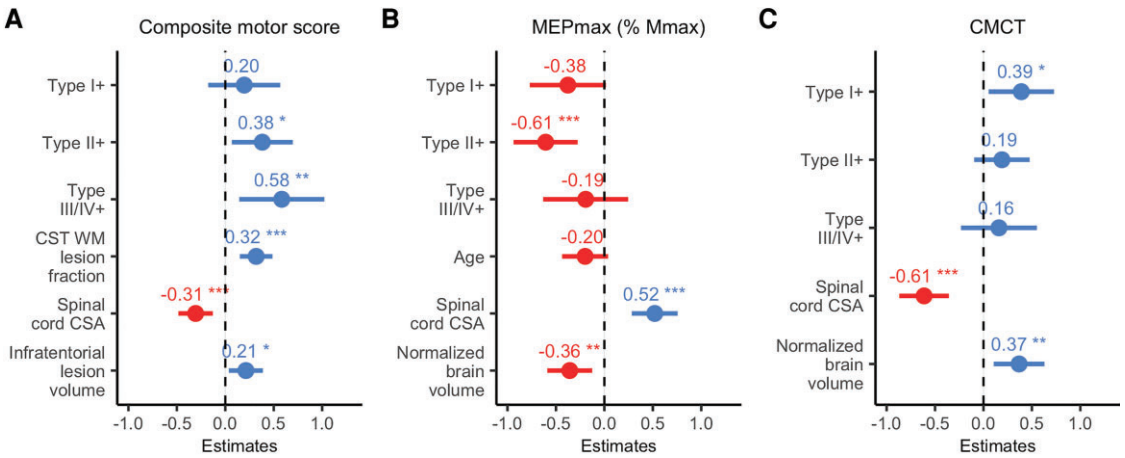

Figure 4 Exploratory stepwise mixed linear regression models of cortical lesion subtypes. Standardized β-coefficients (dots) and 95% standardized CIs of effect size (lines) for each variable included from the stepwise mixed linear regression models. (**A**) Composite motor score; (**B**) MEP_{max}; (**C**) CMCT. Negative and positive values denote a negative and a positive relationship, respectively. $^{*}P < 0.05$, $^{**}P < 0.01$, $^{***}P < 0.001$. WM = white matter; CSA = cross-sectional area.

the presence of a cortical lesion in SM1-HAND was associated with a delay in CMCT [$t(65.53) = 2.87$, $P = 0.005$] (conditional $R^2 = 0.829$).

Stepwise mixed linear regressions were not performed on the RMT and the N20 latency, given the lack of significant group effects in the initial analyses. Running the models substituting whole-brain white matter lesion volume with CST white matter lesion fraction and whole-brain cortical lesion count with whole-brain cortical lesion volume did not change any conclusions from the analyses.

Table 3 Correlations between behaviour and electrophysiology

	Composite motor score	Composite sensory score
CMCT	0.27 ($P = 0.08$)	0.15 ($P = 1$)
SEP	**0.46 ($P < 0.001$)**	**0.47 ($P < 0.001$)**
MEP_{max}	**−0.34 ($P = 0.019$)**	**−0.38 ($P = 0.009$)**
RMT	**0.46 ($P < 0.001$)**	**0.37 ($P = 0.009$)**

Spearman's correlation coefficients and Holm corrected *P*-values. Significant values are highlighted in bold.

Cortical lesion subtypes and hand dysfunction

We performed an exploratory analysis in which we grouped patients based on the presence of cortical lesion subtypes. Modelling lesion subtypes as fixed effects, we found that the relation between CL+ and worse composite motor score was primarily associated with type II intracortical lesions [$t(99.41) = 2.38$, $P = 0.02$] and type III/IV subpial lesions [$t(99.98) = 2.60$, $P = 0.01$]. There was no significant effect of type I lesions ($P = 0.42$; Fig. 4A). For the neurophysiological measures, the statistical effect on MEP_{max} was associated with type II lesions [$t(67.79) = -3.59$, $P = 0.001$], while CMCT delay was primarily associated with type I lesions [$t(51.59) = 2.27$, $P = 0.028$; Fig. 4B and C]. The composite sensory score was not reassessed, because cortical lesions in SM1-HAND had no statistically significant effect after stepwise variable reduction. Neither total nor subtype cortical lesion number or volume correlated with manual sensorimotor dysfunction after adjusting for multiple comparisons ($P > 0.78$; Supplementary Table 3).

Relation between cortical lesion load and clinical disability

EDSS scaled with total and type II cortical lesion number and volume, infratentorial lesion volume and spinal cord atrophy. Correlations between EDSS and electrophysiological measures, averaged over both sides, showed significant correlations with CMCT, N20 latency and MEP_{max}. FSp correlated only with spinal cord atrophy after correcting for multiple comparisons. However, the FSp correlated with all neurophysiological measures. The FSs correlated with total and type I cortical lesion count. In contrast to the FS pyramidal score, the FS sensory score did not correlate with any neurophysiological measures. Motor fatigue scores did not correlate with any MRI or neurophysiological measures. All correlation coefficients are shown in Table 4.

Discussion

In this study we found that the presence of cortical lesions in the highly specialized SM1-HAND area was associated with reduced motor and sensory function of the contralateral hand. Moreover, by investigating domain-specific function in the sensorimotor pathways linking the hand and cortex with TMS and SSEPs we also found that the presence of cortical lesions in SM1-HAND were associated with delayed corticospinal conduction and reduced corticospinal excitability. Importantly, there was still an association between the presence of cortical lesions in SM1-HAND and hand function after accounting for demographic variables and pathway-specific MRI metrics, which contribute to sensorimotor dysfunction in multiple sclerosis.

Cortical lesions are associated with domain-specific functional impairment

To the best of our knowledge, this is the first study investigating the link between the anatomical location of cortical lesions detected with 7 T MRI and their relation to domain-related neurological function. Our findings in relapse-free patients confirm and extend previous observations in case series of patients showing 'cortical relapses', i.e. the acute appearance of symptoms related to the emergence of a cortical lesion.[56] In one study, five RRMS cases were reported, presenting with various symptoms, all relating to a new cortical lesion. One case presented with hypoesthesia of the left arm and later muscle twitching of the hand, arm and face which was linked to a large subpial lesion in the contralateral

Table 4 Correlations with clinical measures of disability and motor fatigue

	EDSS	FS pyramidal	FS sensory	Motor fatigue
Lesion and MRI measures ($n = 50$)				
Total cortical lesion count	**0.40 ($P = 0.046$)**	0.37 ($P = 0.11$)	**0.44 ($P = 0.023$)**	0.10 ($P = 1$)
Type I count	0.33 ($P = 0.13$)	0.24 ($P = 0.42$)	**0.44 ($P = 0.023$)**	0.08 ($P = 1$)
Type II count	**0.41 ($P = 0.039$)**	0.40 ($P = 0.06$)	0.37 ($P = 0.11$)	0.07 ($P = 1$)
Type III/IV count	0.30 ($P = 0.16$)	0.31 ($P = 0.26$)	0.35 ($P = 0.087$)	0.17 ($P = 1$)
Total cortical lesion volume	**0.40 ($P = 0.046$)**	0.31 ($P = 0.34$)	0.38 ($P = 0.12$)	0.06 ($P = 1$)
Type I volume	0.37 ($P = 0.075$)	0.29 ($P = 0.35$)	0.37 ($P = 0.11$)	0.07 ($P = 1$)
Type II volume	**0.40 ($P = 0.046$)**	0.30 ($P = 0.34$)	0.29 ($P = 0.24$)	0.00 ($P = 1$)
Type III/IV volume	0.34 ($P = 0.13$)	0.25 ($P = 0.42$)	0.35 ($P = 0.11$)	0.09 ($P = 1$)
Juxtacortical lesion volume	0.22 ($P = 0.39$)	0.20 ($P = 0.42$)	0.37 ($P = 0.11$)	0.00 ($P = 1$)
WM lesion volume	0.24 ($P = 0.39$)	0.27 ($P = 0.40$)	0.29 ($P = 0.24$)	0.13 ($P = 1$)
Normalized brain volume	−0.32 ($P = 0.15$)	−0.33 ($P = 0.26$)	−0.35 ($P = 0.11$)	−0.19 ($P = 1$)
Spinal cord CSA	**−0.50 ($P = 0.003$)**	**−0.42 ($P = 0.043$)**	−0.28 ($P = 0.24$)	−0.24 ($P = 1$)
Infratentorial lesion volume	**0.41 ($P = 0.04$)**	0.27 ($P = 0.40$)	0.26 ($P = 0.24$)	0.29 ($P = 0.59$)
Mean CST WM lesion fraction	0.22 ($P = 0.39$)	0.25 ($P = 0.42$)	0.24 ($P = 0.24$)	0.12 ($P = 1$)
Mean pericentral thickness	−0.1 ($P = 0.49$)	−0.20 ($P = 0.42$)	−0.19 ($P = 0.24$)	−0.02 ($P = 1$)
Neurophysiological measures ($n = 37$)				
Mean CMCT	**0.50 ($P = 0.005$)**	**0.62 ($P < 0.001$)**	0.11 ($P = 0.98$)	0.21 ($P = 0.72$)
Mean N20 latency	**0.43 ($P = 0.022$)**	**0.52 ($P = 0.004$)**	0.16 ($P = 0.98$)	0.00 ($P = 1$)
Mean MEP_{max}	**−0.47 ($P = 0.009$)**	**−0.64 ($P < 0.001$)**	−0.17 ($P = 0.98$)	−0.23 ($P = 0.72$)
Mean RMT	0.27 ($P = 0.1$)	**0.4 ($P = 0.015$)**	0.22 ($P = 0.78$)	0.09 ($P = 1$)

Significant values are highlighted in bold.

pre- and postcentral sulcus. In another study, seizure activity in a patient with newly developed inferior limb sensory–motor status epilepticus was shown to overlap with a new cortical lesion in the sensory–motor foot area.[57] While these studies are mainly qualitative, the observations suggest a link between cortical lesions and the emergence of acute neurological deficits. Our results further propose a lasting contribution of cortical lesions to non-acute domain-specific functional impairments in relapse-free patients. Our extended analysis showed that the effect of CL+ was most pronounced for the non-dominant hand. One explanation for this could be that continued use of the affected limb ameliorates the detrimental effects of a cortical lesion, potentially through use-dependent plasticity.[58] This could imply that intensified rehabilitation of especially the non-dominant side could be beneficial for patients suffering from motor impairment.

The presence of cortical lesions in contralateral SM1-HAND also associated with sensory performance. Yet, this effect was no longer significant after controlling for other variables that may contribute to sensory dysfunction. Sensory processing may be less susceptible to the presence of cortical lesions, given that sensory input is processed in multiple primary and secondary somatosensory areas.[59] Further, more thorough testing of sensory capabilities, e.g. two-point discrimination, temporal discrimination or position sense, might have yielded a more comprehensive sensory composite score and thereby a more robust relationship with cortical lesions. Future studies should apply more detailed sensory testing, given the strict somatotopic relationship between sensory input and cortical processing.[60,61]

In line with previous MRI studies at 1.5 T,[62] 3 T[63,64] and 7 T,[20,21,25] we found a positive correlation between whole-brain cortical lesion load and EDSS scores, further corroborating the association between cortical involvement and overall disability. Thus, cortical lesions detected at ultra-high field are emerging as a highly relevant pathological marker, which may support the use of whole-brain white-matter lesion volume as non-specific markers of disease activity. However, our results suggest increased specificity of MRI-related pathology when focusing on the neural pathway associated with a particular functional domain. In line with our results, previous studies have also attributed numerous neuroimaging findings, specific to the sensorimotor system, to both global (EDSS)[8–10,65–67] and hand specific disability[8,67,68] along with motor progression of the contralateral limb.[69] Our 7 T MRI data further demonstrate that also lesions in the cortical component of the corticospinal network may contribute to hand motor impairment. Importantly, we were able to show topographical- and domain-related specificity of our results, as cortical lesion presence in the control regions of interest had no effect on the outcome measures. It will be highly interesting for future studies to investigate whether our findings are transferable to other primary cortical domains such as vision or audition.

The exploratory analysis of cortical lesion subtypes suggests that the Group effect on motor performance was primarily driven by intracortical type II and III/IV lesions. This is in contrast to two earlier studies, which found that motor disability was primarily related to whole-brain cortical type I lesions lesion load.[21,22] This discrepancy might reflect the difference in assessing whole-brain versus regional cortical lesion load. Whole-brain type I, but not type II–IV, lesions have been shown to relate to white-matter lesion load[21,70] and may be a stronger indicator of the general disability level of the patient. On the other hand, our data suggest that types II and III/IV lesions have a local influence on the function of the cortical area in which they reside. This notion could be explained by a differential effect of the cortical layer affected by the different lesion types, a hypothesis that requires further investigation.

Lesions in SM1-HAND and corticospinal integrity

Patients with cortical lesions in SM1-HAND showed a reduced TMS-evoked motor response in the contralateral hand along with a longer corticospinal conduction time relative to patients without a lesion in SM1-HAND. The effect size was larger for MEP_{max} than CMCT, and exploratory analyses further suggest that the reduction in MEP_{max} was primarily related to type II intracortical lesions, while the CMCT delay was mainly related to leucocortical lesions. Both inhibitory and excitatory neurons in the primary motor cortex have been shown to be affected by cortical lesions,[71–73] which may lead to faulty activation of cortical output neurons in the CST and could account for the reduction in MEP amplitude. Demyelination has also been suggested to lead to increased refractoriness of axons.[74] This could in turn impair the high-frequency descending volleys that are elicited by TMS,[75] leading to decreased temporal summation at the alpha motoneuron level, measurable as a decrease in the MEP_{max}.

Desynchronization of descending volleys and resulting phase cancellation at the EMG electrode level,[76,77] which is also observed in healthy controls, is substantially increased in multiple sclerosis patients because demyelinating lesions slow down conduction velocity in the CST. In addition, lesions can cause conduction block or axonal loss in the corticospinal system.[78] Dissociating these neurophysiological components was not possible in the current study, and thus, our CMCT and MEP_{max} results are likely driven by overlapping mechanisms. Using a triple stimulation technique[78] could help dissociate these processes in future studies.

Delayed central conduction time most likely reflects partial demyelination of axons in multiple sclerosis.[74] However, our study suggests that cortical lesions, and type I lesions in particular, may also contribute to delaying the CMCT. Due to the relatively small size of cortical lesions, axonal demyelination alone is unlikely to be the sole explanation of this finding. Histopathological studies have described reduced neuronal and synaptic density in type I lesions[79] and grey-matter lesions in general.[80] Whether neuronal loss or transection is specific to fast-conducting output neurons in the motor cortex is unknown, but it may be a contributor to the conduction time delays observed in the current study.

In contrast to the motor system, we only found a trend towards a Group effect of delayed somatosensory conduction times in CL+ patients. This lack of effect may reflect the difference in specificity of the motor and sensory system. While TMS most likely activates pyramidal tract neurons from both the primary motor, but also premotor and sensory cortices,[81,82] digital nerve stimulation of a single finger elicits a highly selective cortical response.[61] It is thus likely that our relatively large cortical region of interest of SM1-HAND was not selective enough to express a clear link with the probed sensory modality. However, it should be noted that all patients with a substantially delayed N20 latency were in the CL+ group (Fig. 2F).

Limitations

The cross-sectional study design limits the causal interpretations of SM1-HAND cortical lesions on behavioural and neurophysiological outcomes. Damage caused by cortical lesions may be more severe in acute states and may be partially compensated by cortical plasticity and remyelination,[58,83] which limits the sensitivity of our analyses. Although neurobiologically plausible, the causal relevance of our findings and their generalizability to other cortical areas needs to be corroborated in future longitudinal studies.

Although the introduction of 7 T MRI has substantially improved the detection of cortical lesions, 7 T MRI still does not capture the

full extent of cortical damage and differentiation among lesion subtypes remains challenging. We identified a mean cortical lesion number per patient in line with previous 7 T studies,[19,21,24] but we observed a larger proportion of type II intracortical lesions than previously described with MRI[24,25] and histology.[16,79,84] It might be that our population of patients exhibited a large amount of type II lesions. However, it might also be due to a systematic misclassification of type III/IV as type II lesions. Including a T_2^*-weighted sequence, which has been suggested to be more sensitive towards subpial lesions,[25] could be beneficial in future studies. The MP2RAGE sequence also seems sensitive towards cortical lesions.[85] However, lesion segmentation with the MP2RAGE sequence in this study was hampered by data export and image-processing complications during the lesion segmentation process.

Due to the limited field of view achievable with the 7 T head coil used in our study, we were not able to detect spinal cord lesions, which have been identified as relevant structural markers of motor disability.[65,86] We were, however, able to assess spinal cord atrophy at the C1–C2 level, which proved to be highly sensitive towards our outcome measures.

Clinical data from patients were acquired up to 3 months prior to participation, which might have had some impact on EDSS and FSMC scores. However, as only relapse-free patients were recruited and no relapses were reported during participation, this is most likely to have affected data from our SPMS cohort ($n = 13$).

Lastly, it is important to note that the SM1-HAND is embedded in a cortico-subcortical motor network, including other sensorimotor areas in the frontal and parietal cortex, basal ganglia, thalamus and cerebellum.[87,88] Taking a broader network perspective that considers additional lesions in non-primary, sensorimotor, cortical areas might have revealed an even stronger impact of cortical lesions on manual motor control.

Conclusion

In this study, the comprehensive multilevel assessment of sensorimotor brain damage and dysfunction linked the presence of cortical lesions in SM1-HAND on 7 T MRI scans to hand disability. Moreover, the TMS measurements showed that the SM1-HAND containing a cortical lesion was associated with measures of reduced corticospinal conduction and excitability. Importantly, these effects were still present after considering other MRI metrics of subcortical CST damage and were spatially specific to the contralateral SM1-HAND. Our results also provide preliminary evidence that various facets of corticomotor control of the contralateral hand may display difference in their susceptibility to the type of cortical lesion.

Acknowledgements

We would like to thank all the patients and healthy controls who have participated in this project, for their essential support to our research. We would also like to thank Sascha Gude, Helena-Céline Stevelt and Jasmin Merhout for contributing with lesion segmentation and quality assurance of MRI data.

Funding

This study was funded by the Danish Multiple Sclerosis Society [A31942; A33409; A35202; A38506], the independent research fund Denmark [9039-00330B], Gangstedfonden [A38060], and Copenhagen University Hospital Amager & Hvidovre. The 7 T scanner was donated by the John and Birthe Meyer Foundation and The Danish Agency for Science, Technology and Innovation [0601-01370B]. H.R.S. holds a 5-year professorship in precision medicine at the Faculty of Health Sciences and Medicine, University of Copenhagen, sponsored by the Lundbeck Foundation [R186-2015-2138]. V.W. is supported by the Danish Multiple Sclerosis Society [A40219] and the Lundbeck Foundation [R347-2020-2413]. H.L is supported by the European Research Council (ERC) under the European Union's Horizon 2020 research and innovation programme (grant agreement No 804746). S.C. has received funding from the Horizon 2020 Framework Programme grant agreement No 765148.

Competing interests

M.A.J.M., M.F.M.M., V.W., S.C. and O.P. report no competing interests. H.R.S. has received honoraria as speaker from Sanofi Genzyme, Denmark and Novartis, Denmark, as consultant for Sanofi Genzyme, Denmark, Lophora, Denmark and Lundbeck AS, Denmark, and as editor-in-chief (*Neuroimage Clinical*) and senior editor (*NeuroImage*) from Elsevier Publishers, Amsterdam, The Netherlands. He has received royalties as book editor from Springer Publishers, Stuttgart, Germany and from Gyldendal Publishers, Copenhagen, Denmark. H.L. is inventor on two patent applications with royalty agreement with RWI AB, Lund, Sweden. F.S. has served on scientific advisory boards for, served as consultant for, received support for congress participation or received speaker honoraria from Alexion, Biogen, Bristol Myers Squibb, H. Lundbeck A/S, Merck, Novartis, Roche and Sanofi Genzyme. His laboratory has received research support from Biogen, Merck, Novartis, Roche and Sanofi Genzyme. J.R.C. has received speaker honoraria from Biogen. M.B. has served on scientific advisory boards for Sanofi-Genzyme, Roche, Biogen, Merck, Novartis and Teva; has received speaker honoraria from Sanofi-Genzyme, Biogen, Merck, Novartis, Teva and Roche; has received consulting honoraria from the Danish Multiple Sclerosis Society, Sanofi-Genzyme, Biogen, Teva, Roche and Merck; and has received funding for travel from Sanofi-Genzyme, Roche, Teva and Biogen.

Supplementary material

Supplementary material is available at *Brain* online.

References

1. Reich DS, Lucchinetti CF, Calabresi PA. Multiple sclerosis. *N Engl J Med*. 2018;378:169–180.
2. Wattjes MP, Rovira A, Miller D, *et al*. Evidence-based guidelines: MAGNIMS consensus guidelines on the use of MRI in multiple sclerosis—Establishing disease prognosis and monitoring patients. *Nat Rev Neurol*. 2015;11:597–606.
3. Barkhof F. MRI In multiple sclerosis: Correlation with Expanded Disability Status Scale (EDSS). *Mult Scler*. 1999;5:283–286.
4. Bermel RA, Bakshi R. The measurement and clinical relevance of brain atrophy in multiple sclerosis. *Lancet Neurol*. 2006;5:158–170.
5. Steenwijk MD, Geurts JJ, Daams M, *et al*. Cortical atrophy patterns in multiple sclerosis are non-random and clinically relevant. *Brain*. 2016;139:115–126.
6. Sailer M, Fischl B, Salat D, *et al*. Focal thinning of the cerebral cortex in multiple sclerosis. *Brain*. 2003;126:1734–1744.

7. Casserly C, Seyman EE, Alcaide-Leon P, *et al*. Spinal cord atrophy in multiple sclerosis: A systematic review and meta-analysis. *J Neuroimaging*. 2018;28:556–586.
8. Daams M, Steenwijk MD, Wattjes MP, *et al*. Unraveling the neuroimaging predictors for motor dysfunction in long-standing multiple sclerosis. *Neurology*. 2015;85:248–255.
9. Kerbrat A, Gros C, Badji A, *et al*. Multiple sclerosis lesions in motor tracts from brain to cervical cord: Spatial distribution and correlation with disability. *Brain*. 2020;143:2089–2105.
10. Cordani C, Hidalgo de la Cruz M, Meani A, *et al*. MRI Correlates of clinical disability and hand-motor performance in multiple sclerosis phenotypes. *Mult Scler*. 2021;27:1205–1221.
11. Barkhof F. The clinico-radiological paradox in multiple sclerosis revisited. *Curr Opin Neurol*. 2002;15:239–245.
12. Lucchinetti CF, Popescu BF, Bunyan RF, *et al*. Inflammatory cortical demyelination in early multiple sclerosis. *N Engl J Med*. 2011;365:2188–2197.
13. Seewann A, Kooi EJ, Roosendaal SD, *et al*. Postmortem verification of MS cortical lesion detection with 3D DIR. *Neurology*. 2012;78:302–308.
14. Bouman PM, Steenwijk MD, Pouwels PJW, *et al*. Histopathology-validated recommendations for cortical lesion imaging in multiple sclerosis. *Brain*. 2020;143:2988–2997.
15. Kraff O, Quick HH. 7T: Physics, safety, and potential clinical applications. *J Magn Reson Imaging*. 2017;46:1573–1589.
16. Kilsdonk ID, Jonkman LE, Klaver R, *et al*. Increased cortical grey matter lesion detection in multiple sclerosis with 7 T MRI: A post-mortem verification study. *Brain*. 2016;139:1472–1481.
17. Nielsen AS, Kinkel RP, Tinelli E, Benner T, Cohen-Adad J, Mainero C. Focal cortical lesion detection in multiple sclerosis: 3 Tesla DIR versus 7 tesla FLASH-T2. *J Magn Reson Imaging*. 2012;35:537–542.
18. Beck ES, Gai N, Filippini S, Maranzano J, Nair G, Reich DS. Inversion recovery susceptibility weighted imaging with enhanced T2 weighting at 3 T improves visualization of subpial cortical multiple sclerosis lesions. *Invest Radiol*. 2020;55:727–735.
19. Madsen MAJ, Wiggermann V, Bramow S, Christensen JR, Sellebjerg F, Siebner HR. Imaging cortical multiple sclerosis lesions with ultra-high field MRI. *Neuroimage Clin*. 2021;32:102847.
20. Nielsen AS, Kinkel RP, Madigan N, Tinelli E, Benner T, Mainero C. Contribution of cortical lesion subtypes at 7 T MRI to physical and cognitive performance in MS. *Neurology*. 2013;81:641–649.
21. Harrison DM, Roy S, Oh J, *et al*. Association of cortical lesion burden on 7-T magnetic resonance imaging with cognition and disability in multiple sclerosis. *JAMA Neurol*. 2015;72:1004–1012.
22. Cocozza S, Cosottini M, Signori A, *et al*. A clinically feasible 7-tesla protocol for the identification of cortical lesions in multiple sclerosis. *Eur Radiol*. 2020;30:4586–4594.
23. Louapre C, Govindarajan ST, Gianni C, *et al*. Heterogeneous pathological processes account for thalamic degeneration in multiple sclerosis: Insights from 7 T imaging. *Mult Scler*. 2018;24:1433–1444.
24. Mehndiratta A, Treaba CA, Barletta V, *et al*. Characterization of thalamic lesions and their correlates in multiple sclerosis by ultra-high-field MRI. *Mult Scler*. 2021:27:674–683.
25. Mainero C, Benner T, Radding A, *et al*. *In vivo* imaging of cortical pathology in multiple sclerosis using ultra-high field MRI. *Neurology*. 2009;73:941–948.
26. Treaba CA, Granberg TE, Sormani MP, *et al*. Longitudinal characterization of cortical lesion development and evolution in multiple sclerosis with 7.0-T MRI. *Radiology*. 2019;291:740–749.
27. Pisani AI, Scalfari A, Crescenzo F, Romualdi C, Calabrese M. A novel prognostic score to assess the risk of progression in relapsing–remitting multiple sclerosis patients. *Eur J Neurol*. 2021;28:2503–2512.
28. Scalfari A, Romualdi C, Nicholas RS, *et al*. The cortical damage, early relapses, and onset of the progressive phase in multiple sclerosis. *Neurology*. 2018;90:e2107–e2118.
29. Simpson M, Macdonell R. The use of transcranial magnetic stimulation in diagnosis, prognostication and treatment evaluation in multiple sclerosis. *Mult Scler Relat Disord*. 2015;4:430–436.
30. Yousry TA, Schmid UD, Alkadhi H, *et al*. Localization of the motor hand area to a knob on the precentral gyrus. A new landmark. *Brain*. 1997;120:141–157.
31. Rossi S, Hallett M, Rossini PM, Pascual-Leone A; Safety of TMS Consensus Group. Safety, ethical considerations, and application guidelines for the use of transcranial magnetic stimulation in clinical practice and research. *Clin Neurophysiol*. 2009;120:2008–2039.
32. Andersen M, Bjorkman-Burtscher IM, Marsman A, Petersen ET, Boer VO. Improvement in diagnostic quality of structural and angiographic MRI of the brain using motion correction with interleaved, volumetric navigators. *PLoS One*. 2019;14:e0217145.
33. Ganzetti M, Wenderoth N, Mantini D. Quantitative evaluation of intensity inhomogeneity correction methods for structural MR brain images. *Neuroinformatics*. 2016;14:5–21.
34. Avants BB, Tustison N, Johnson H. Advanced normalization tools (ANTS). *Insight J*. 2014;2:1–35.
35. Geurts JJ, Roosendaal SD, Calabrese M, *et al*. Consensus recommendations for MS cortical lesion scoring using double inversion recovery MRI. *Neurology*. 2011;76:418–424.
36. Granberg T, Fan Q, Treaba CA, *et al*. *In vivo* characterization of cortical and white matter neuroaxonal pathology in early multiple sclerosis. *Brain*. 2017;140:2912–2926.
37. Herranz E, Gianni C, Louapre C, *et al*. Neuroinflammatory component of gray matter pathology in multiple sclerosis. *Ann Neurol*. 2016;80:776–790.
38. Bø L, Vedeler CA, Nyland HI, Trapp BD, Mork SJ. Subpial demyelination in the cerebral cortex of multiple sclerosis patients. *J Neuropathol Exp Neurol*. 2003;62:723–732.
39. Puonti O, Iglesias JE, Van Leemput K. Fast and sequence-adaptive whole-brain segmentation using parametric Bayesian modeling. *Neuroimage*. 2016;143:235–249.
40. Cerri S, Puonti O, Meier DS, *et al*. A contrast-adaptive method for simultaneous whole-brain and lesion segmentation in multiple sclerosis. *Neuroimage*. 2021;225:117471.
41. Jenkinson M, Beckmann CF, Behrens TE, Woolrich MW, Smith SM. Fsl. *Neuroimage*. 2012;62:782–790.
42. Tournier JD, Smith R, Raffelt D, *et al*. MRtrix3: A fast, flexible and open software framework for medical image processing and visualisation. *Neuroimage*. 2019;202:116137.
43. Veraart J, Novikov DS, Christiaens D, Ades-Aron B, Sijbers J, Fieremans E. Denoising of diffusion MRI using random matrix theory. *Neuroimage*. 2016;142:394–406.
44. Andersson JL, Skare S, Ashburner J. How to correct susceptibility distortions in spin-echo echo-planar images: Application to diffusion tensor imaging. *Neuroimage*. 2003;20:870–888.
45. Andersson JLR, Graham MS, Drobnjak I, Zhang H, Filippini N, Bastiani M. Towards a comprehensive framework for movement and distortion correction of diffusion MR images: Within volume movement. *Neuroimage*. 2017;152:450–466.
46. Wasserthal J, Neher P, Maier-Hein KH. Tractseg—Fast and accurate white matter tract segmentation. *Neuroimage*. 2018;183:239–253.
47. De Leener B, Levy S, Dupont SM, *et al*. SCT: Spinal cord toolbox, an open-source software for processing spinal cord MRI data. *Neuroimage*. 2017;145:24–43.
48. Feys P, Lamers I, Francis G, *et al*. The Nine-Hole Peg Test as a manual dexterity performance measure for multiple sclerosis. *Mult Scler*. 2017;23:711–720.

49. Jebsen RH, Taylor N, Trieschmann RB, Trotter MJ, Howard LA. An objective and standardized test of hand function. *Arch Phys Med Rehabil*. 1969;50:311–319.
50. Penner IK, Raselli C, Stocklin M, Opwis K, Kappos L, Calabrese P. The fatigue scale for motor and cognitive functions (FSMC): Validation of a new instrument to assess multiple sclerosis-related fatigue. *Mult Scler*. 2009;15:1509–1517.
51. Oldfield RC. The assessment and analysis of handedness: The Edinburgh inventory. *Neuropsychologia*. 1971;9:97–113.
52. Van Boven RW, Johnson KO. The limit of tactile spatial resolution in humans: Grating orientation discrimination at the lip, tongue, and finger. *Neurology*. 1994;44:2361–2366.
53. Ragert P, Vandermeeren Y, Camus M, Cohen LG. Improvement of spatial tactile acuity by transcranial direct current stimulation. *Clin Neurophysiol*. 2008;119:805–811.
54. Groppa S, Oliviero A, Eisen A, *et al*. A practical guide to diagnostic transcranial magnetic stimulation: Report of an IFCN committee. *Clin Neurophysiol*. 2012;12:858–882.
55. Rossini PM, Burke D, Chen R, *et al*. Non-invasive electrical and magnetic stimulation of the brain, spinal cord, roots and peripheral nerves: Basic principles and procedures for routine clinical and research application. An updated report from an I.F.C.N. Committee. *Clin Neurophysiol*. 2015;126:1071–1107.
56. Puthenparampil M, Poggiali D, Causin F, *et al*. Cortical relapses in multiple sclerosis. *Mult Scler*. 2016;22:1184–1191.
57. Gasparini E, Benuzzi F, Pugnaghi M, *et al*. Focal sensory–motor status epilepticus in multiple sclerosis due to a new cortical lesion. An EEG-fMRI co-registration study. *Seizure*. 2010;19:525–528.
58. Zeller D, Classen J. Plasticity of the motor system in multiple sclerosis. *Neuroscience*. 2014;283:222–230.
59. McGlone F, Kelly EF, Trulsson M, Francis ST, Westling G, Bowtell R. Functional neuroimaging studies of human somatosensory cortex. *Behav Brain Res*. 2002;135:147–158.
60. Mima T, Ikeda A, Terada K, *et al*. Modality-specific organization for cutaneous and proprioceptive sense in human primary sensory cortex studied by chronic epicortical recording. *Electroencephalogr Clin Neurophysiol*. 1997;104:103–107.
61. Sanchez Panchuelo RM, Ackerley R, Glover PM, *et al*. Mapping quantal touch using 7 tesla functional magnetic resonance imaging and single-unit intraneural microstimulation. *Elife*. 2016;5:e12812.
62. Calabrese M, Rocca MA, Atzori M, *et al*. A 3-year magnetic resonance imaging study of cortical lesions in relapse-onset multiple sclerosis. *Ann Neurol*. 2010;67:376–383.
63. Mike A, Glanz BI, Hildenbrand P, *et al*. Identification and clinical impact of multiple sclerosis cortical lesions as assessed by routine 3 T MR imaging. *AJNR Am J Neuroradiol*. 2011;32:515–521.
64. Sethi V, Yousry TA, Muhlert N, *et al*. Improved detection of cortical MS lesions with phase-sensitive inversion recovery MRI. *J Neurol Neurosurg Psychiatry*. 2012;83:877–882.
65. Chouteau R, Combes B, Bannier E, *et al*. Joint assessment of brain and spinal cord motor tract damage in patients with early RRMS: Predominant impact of spinal cord lesions on motor function. *J Neurol*. 2019;266:2294–2303.
66. Bodini B, Battaglini M, De Stefano N, *et al*. T2 lesion location really matters: A 10 year follow-up study in primary progressive multiple sclerosis. *J Neurol Neurosurg Psychiatry*. 2011;82:72–77.
67. Kearney H, Altmann DR, Samson RS, *et al*. Cervical cord lesion load is associated with disability independently from atrophy in MS. *Neurology*. 2015;84:367–373.
68. Ouellette R, Treaba CA, Granberg T, *et al*. 7 T imaging reveals a gradient in spinal cord lesion distribution in multiple sclerosis. *Brain*. 2020;143:2973–2987.
69. Sechi E, Keegan BM, Kaufmann TJ, Kantarci OH, Weinshenker BG, Flanagan EP. Unilateral motor progression in MS: Association with a critical corticospinal tract lesion. *Neurology*. 2019;93:e628–e634.
70. Beck ES, Maranzano J, Luciano NJ, *et al*. Cortical lesion hotspots and association of subpial lesions with disability in multiple sclerosis. *Mult Scler*. 2022;28(9):1351–1363.
71. Magliozzi R, Pitteri M, Ziccardi S, *et al*. CSF Parvalbumin levels reflect interneuron loss linked with cortical pathology in multiple sclerosis. *Ann Clin Transl Neurol*. 2021;8:534–547.
72. Schirmer L, Velmeshev D, Holmqvist S, *et al*. Neuronal vulnerability and multilineage diversity in multiple sclerosis. *Nature*. 2019;573:75–82.
73. Zoupi L, Booker SA, Eigel D, *et al*. Selective vulnerability of inhibitory networks in multiple sclerosis. *Acta Neuropathol*. 2021;141:415–429.
74. Smith KJ. Conduction properties of central demyelinated and remyelinated axons, and their relation to symptom production in demyelinating disorders. *Eye (Lond)*. 1994;8:224–237.
75. Di Lazzaro V, Oliviero A, Mazzone P, *et al*. Generation of I waves in the human: Spinal recordings. *Suppl Clin Neurophysiol*. 2003;56:143–152.
76. Rosler KM, Petrow E, Mathis J, Aranyi Z, Hess CW, Magistris MR. Effect of discharge desynchronization on the size of motor evoked potentials: An analysis. *Clin Neurophysiol*. 2002;113:1680–1687.
77. Magistris M. Transcranial stimulation excites virtually all motor neurons supplying the target muscle. A demonstration and a method improving the study of motor evoked potentials. *Brain*. 1998;121:437–450.
78. Magistris MR, Rosler KM, Truffert A, Landis T, Hess CW. A clinical study of motor evoked potentials using a triple stimulation technique. *Brain*. 1999;122:265–279.
79. Wegner C, Esiri MM, Chance SA, Palace J, Matthews PM. Neocortical neuronal, synaptic, and glial loss in multiple sclerosis. *Neurology*. 2006;67:960–967.
80. Vercellino M, Marasciulo S, Grifoni S, *et al*. Acute and chronic synaptic pathology in multiple sclerosis gray matter. *Mult Scler*. 2022:28:369–382.
81. Reijonen J, Pitkanen M, Kallioniemi E, Mohammadi A, Ilmoniemi RJ, Julkunen P. Spatial extent of cortical motor hotspot in navigated transcranial magnetic stimulation. *J Neurosci Methods*. 2020;346:108893.
82. Aberra AS, Wang B, Grill WM, Peterchev AV. Simulation of transcranial magnetic stimulation in head model with morphologically-realistic cortical neurons. *Brain Stimul*. 2020;13:175–189.
83. Chang A, Staugaitis SM, Dutta R, *et al*. Cortical remyelination: A new target for repair therapies in multiple sclerosis. *Ann Neurol*. 2012;72:918–926.
84. Peterson JW, Bo L, Mork S, Chang A, Trapp BD. Transected neurites, apoptotic neurons, and reduced inflammation in cortical multiple sclerosis lesions. *Ann Neurol*. 2001;50:389–400.
85. Beck ES, Sati P, Sethi V, *et al*. Improved visualization of cortical lesions in multiple sclerosis using 7 T MP2RAGE. *AJNR Am J Neuroradiol*. 2018;39:459–466.
86. Arrambide G, Rovira A, Sastre-Garriga J, *et al*. Spinal cord lesions: A modest contributor to diagnosis in clinically isolated syndromes but a relevant prognostic factor. *Mult Scler*. 2018;24:301–312.
87. Borra E, Luppino G. Large-scale temporo-parieto-frontal networks for motor and cognitive motor functions in the primate brain. *Cortex*. 2019;118:19–37.
88. Bedard P, Sanes JN. Brain representations for acquiring and recalling visual–motor adaptations. *Neuroimage*. 2014;101:225–235.